

AperTO - Archivio Istituzionale Open Access dell'Università di Torino

Accuracy assessment of the CNAO dose delivery system in the initial period of clinical activity and impact of later improvements on delivered dose distributions

This is the author's manuscript

Original Citation:

Availability:

This version is available <http://hdl.handle.net/2318/1757601> since 2020-10-02T12:26:13Z

Published version:

DOI:10.1002/mp.14040

Terms of use:

Open Access

Anyone can freely access the full text of works made available as "Open Access". Works made available under a Creative Commons license can be used according to the terms and conditions of said license. Use of all other works requires consent of the right holder (author or publisher) if not exempted from copyright protection by the applicable law.

(Article begins on next page)

Title: Accuracy assessment of the CNAO Dose Delivery System in the initial period of clinical activity and impact of later improvements on delivered dose distributions

Short running title: CNAO DDS accuracy assessment

Authors. Anna Vignati^{1,2*}, Seyed Mohammad Amin Hosseini³, Andrea Attili⁴, Mario Ciocca⁵, Marco Donetti⁵, Simona Giordanengo², Flavio Marchetto², Felix Mas Milian^{1,6}, Vincenzo Monaco^{1,2}, Germano Russo^{2†}, Roberto Sacchi^{1,2}, Roberto Cirio^{1,2}

(1)Università degli Studi di Torino, Torino, Italy (2)INFN - National Institute for Nuclear Physics, Torino, Italy (3)Ionizing and Non-Ionizing Radiation Protection Research Center (INIRPRC), Shiraz University of Medical Sciences, Shiraz, Iran (4)INFN - National Institute for Nuclear Physics, Roma, Italy (5)CNAO - National Center for Oncological Hadrontherapy, Pavia, Italy (6)Universidade Estadual de Santa Cruz, Ilheus, Brazil

[†]now at EuriX, Torino, Italy

*first and corresponding author, anna.vignati@to.infn.it, National Institute for Nuclear Physics, via P. Giuria 1, Torino, Italy

Abstract

Purpose: The retrospective analysis of the Dose Delivery System (DDS) performances of the initial clinical operation at CNAO (Centro Nazionale di Adroterapia Oncologica) is reported, and compared with the dose delivery accuracy following the implementation of a position feedback control.

Methods: Log files and raw data of the DDS were analyzed for every field of patients treated with protons and carbon ions between 01/2012 and 04/2013 (~3800 fields). To investigate the DDS accuracy, the spot positions and the number of particles per spot measured by the DDS and prescribed by the Treatment Planning System were compared for each field.

The impact of deviations on dose distributions was studied by comparing, through the gamma-index method, two 3D physical dose maps (one for prescribed, one for measured data), generated by a validated dose computation software. The maximum gamma and the percentage of points with

25 $\gamma \leq 1$ (passing volume) were studied as a function of the treatment day, and correlated with the
26 deviations from the prescription in the measured number of particles and spot positions. Finally,
27 delivered dose distributions of same treatment plans were compared before and after the
28 implementation of a feedback algorithm for the correction of small position deviations, to study the
29 effect on the delivery quality.

30 The double comparison of prescribed and measured 3D maps, before and after feedback
31 implementation, is reported and studied for a representative treatment delivered in 2012, re-delivered
32 on a PMMA block in 2018.

33 **Results.** Systematic deviations of spot positions, mainly due to beam lateral offsets, were always
34 found within 1.5 mm, with the exception of the initial clinical period. The number of particles was
35 very stable, as possible deviations are exclusively related to the quantization error in the conversion
36 from monitor counts to particles. For the chosen representative patient treatment, the gamma-index
37 evaluation of prescribed and measured dose maps, before and after feedback implementation, showed
38 a higher variability of maximum gamma for the 2012 irradiation, with respect to the re-irradiation of
39 2018. However, the 2012 passing volume is $> 99.8\%$ for the sum of all fields, which is comparable
40 to the value of 2018, with the exception of one day with 98.2% passing volume, probably related to
41 an instability of the accelerating system.

42 **Conclusions.** A detailed retrospective analysis of the DDS performances in the initial period of
43 CNAO clinical activity is reported. The spot position deviations are referable to beam lateral offset
44 fluctuations, while almost no deviation was found in the number of particles. The impact of deviations
45 on dose distributions showed that the position feedback implementation and the increased beam
46 control capability acquired after the first years of clinical experience lead to an evident improvement
47 in the DDS stability, evaluated in terms of gamma-index as measure of the impact on dose
48 distributions. However, the clinical effect of the maximum gamma variability found in the 2012
49 representative irradiation is mitigated by averaging along the number of fractions, and the high

percentage of passing volumes confirmed the accuracy of the delivery even before the feedback implementation.

Keywords: charged particle therapy, pencil beam scanning, dose delivery accuracy

Introduction

The first Italian hospital-based charged particle therapy facility (Centro Nazionale di Adroterapia Oncologica, CNAO, Pavia) started clinical activity with protons in September 2011 and one year later with carbon ions, and treated more than 2500 patients at the time of this writing.

The full 3D dose delivery is provided by a dedicated synchrotron with modulated scanning ion beam technique (*pencil beam scanning*), consisting of superposition of thousands of pencil beams of different directions and energies.

During the treatment planning process, the target volume is segmented into iso-energetic layers at different water equivalent depths in tissue. At the time of dose delivery, the layers are scanned by a sequence of pristine beams, named *spots* in the following, of discrete energy, necessary to deposit the required dose at the desired depth, delivering for each spot a defined number of particles at a specific position¹.

To guarantee the irradiation of each spot with the prescribed properties, a dose delivery system (DDS) is needed to monitor and control the beam position and the number of delivered particles for each spot, to control the steering magnets used to scan the treated volume laterally, and to control the sequence of spills provided by the accelerator².

The results of the first year of treatment at CNAO have been already reported from the clinical point of view³ and from the one of patient-specific quality assurance (QA) checks⁴, while a detailed study of the accuracy and performance of the DDS has never been reported so far and it is therefore the object of the present work.

73 It is well-known that the highly conformal dose distribution achieved with active scanned pencil
74 beams has its counterpart in intrinsic sensitivity to delivery uncertainties, and that the accurate
75 delivery of the treatment as prescribed by the treatment planning system (TPS) is crucial to achieve
76 the desired clinical outcomes⁵.

77 The main effort in reducing uncertainties is routinely focused on patient-related sources of errors, i.e.
78 repositioning, related setup imaging, immobilization techniques, identifying anatomical changes and
79 consequently adapting plans⁶. Moreover, daily checks and corrections, if needed, are performed to
80 control potential systematic effects in pencil beam position, size and energy, as well as on the number
81 of delivered particles⁷.

82 Omitting the aforementioned uncertainties due to patient positioning, anatomical changes, and
83 residual systematic effects, particle beam scanning systems deliver the dose with a degree of accuracy
84 depending on the accuracy of position, energy and intensity of the beam extracted from the accelerator
85 and delivered to the target. In addition, finite scan speeds, beam intensity non-uniformities, beam
86 monitoring constraints, and magnet operations all contribute to the inaccuracy of the delivery⁸.

87 The effect of variable machine performance on delivery quality and on the other inaccuracies of the
88 delivery system can be studied through the careful analysis of treatment log files^{9,10}. These files
89 contain the record of the machine parameters for a given field delivery of a given fraction, consisting
90 in the measured positions and measured charge of the monitor chambers, expressed in terms of
91 monitor counts, for each spot^{10,11}. Previous studies have demonstrated that treatment log files created
92 by spot scanning beam delivery systems can be used to determine the inaccuracies of the delivered
93 fraction^{10,11}, providing a thorough understanding of the performance of the system and its stability in
94 time².

95 The aim of this work is twofold: it first reports the dose delivery accuracy of the first 15 months of
96 clinical operation at CNAO and secondly it compares it with the dose delivery accuracy achieved
97 after the system upgrade. This comparison is performed in terms of the impact on the dose

distributions, to evaluate the improvement resulting from the implementation of a beam position feedback algorithm inside the DDS. This work exploited the rare opportunity of having full access to TPS data, treatment plans and DDS data (raw data of monitor chambers and treatment log files). The first goal has been achieved by using the treatment log files to compare prescribed number of particles per spot and spot positions with corresponding measured quantities, for every field of patients treated between January 2012 and April 2013 (more than 3800 fields) with protons and carbon ions. To evaluate the impact on dose distributions of deviations between prescribed and measured quantities, TPS reference values and corresponding values measured by monitor chambers were used as input of a validated dose calculation tool¹². The correspondence between the 3D dose maps has been quantified by means of the gamma-index criterion¹³, and the results have been reported for one representative patient treated with protons. Finally, to study the effect on delivery quality of the implementation of a feedback algorithm for the correction of small position deviations, delivered dose distributions of the same treatment plans before and after feedback implementation have been compared. To this aim, the same representative treatment was repeated on a PMMA block used to dump the beam, and the dose comparison was performed with the acquired data.

Materials and Methods

Brief overview of the CNAO Beam Line

The CNAO synchrotron accelerates ions to a range of kinetic energies (60–250 MeV for protons, 120–400 MeV/u for carbon ions) corresponding to depths in water from 30 to 320 mm for protons and from 30 to 270 mm for carbon ions, with steps of 2 mm for both¹⁴.

Three treatment rooms are available at CNAO, two with horizontal fixed beam line (room 1 and room 3) and the third one with both horizontal and vertical fixed lines (room 2), resulting in 4 independent beam lines and dose delivery systems¹⁴.

121 After the extraction at selected energy from the synchrotron, the particles are sent to the appropriate
 122 beam line to reach the desired treatment room. The last two magnetic elements along the line are two
 123 identical dipole magnets, located approximately 5.5 m upstream the isocenter, to scan horizontally
 124 and vertically each layer of the target volume with the pencil beam scanning approach.

125 The commercial Syngo RT Planning TPS (Siemens AG Healthcare, Erlangen, Germany), is used for
 126 plan optimization and calculation, and the DDS guides the irradiation according to the sequence of
 127 spots defined by the TPS.

128 The DDS in use at CNAO has been designed, built, and commissioned by CNAO, Istituto Nazionale
 129 di Fisica Nucleare (INFN) and University of Torino. Its main components are two independent beam
 130 monitoring detectors, called BOX1 and BOX2, placed downstream the vacuum exit window of the
 131 beam line, interfaced with two control systems performing real-time fast and slow control, and
 132 connected, among others, to the scanning magnets and to a beam chopper. BOX1 consists of a large-
 133 area parallel plate ionization chamber (240x240 mm² sensitive area) to measure the number of beam
 134 particles and two strip chambers (128 strips with a pitch of 1.65 mm) to measure the beam position,
 135 while BOX2 consists of the same large-area parallel plate chamber of BOX1 and a pixel chamber
 136 (32x32 pixels with a pitch of 6.6 mm) used for redundancy.

137 A comprehensive description of the components, essential tasks and operations performed by the
 138 DDS has been reported by Giordanengo et al².

139 Treatment Planning System to Dose Delivery data conversion

140 The TPS groups spots with the same energy into a single slice and generates a plan with all the fields
 141 to irradiate, specified in terms of particles per spot and 2D spot positions (x-y, in mm) for the different
 142 iso-energy layers in the target volume. At each treatment session, patient treatment data are sent to
 143 the dose delivery controller as a text file, through the Mosaic (Elekta, Sunnyvale, USA) Oncology
 144 Information System (OIS) and a custom interface. Before the treatment delivery, plan data are

converted by the DDS into number of monitor counts, position in strips units on the plane of the strip chambers and the scanning magnet currents are calculated as a function of requested energy (in power supply current units).

During the delivery, the data from the monitor chambers acquired by the DDS are used to check the beam position, the number of delivered particles and to control the magnets and the accelerator at the end of each spot and slice, respectively. At the end of each treatment delivery, these raw data are used to create the required treatment record and stored to be used later for the off-line analysis. These data contain for each spot the measured average beam position and the corresponding monitor counts. A reversed conversion into the format of the TPS parameters is applied to the DDS measurements to provide the treatment log file in the proper units for direct comparison with the prescriptions within the OIS.

The data conversion procedure between DDS and TPS data is described in detail in Giordanengo et al.² and is shortly summarized in the following.

Number of particles vs number of monitor counts. The amount of charge released in the gas by particles interaction is measured in real-time by large-area parallel plate ionization chambers¹⁵ and saved in monitor counts spot by spot, where each count refers to a minimum collected charge of 200 fC. This charge quantum corresponds, as an example in a particular nozzle of CNAO and at reference conditions for temperature and pressure, to a number of protons ranging from 7.2×10^3 at the energy of 62 MeV to 1.9×10^4 at the energy of 226 MeV; similarly, the range of the number of carbon ions extends from 341 at the energy of 115 MeV/u to 767 at 399 MeV/u. This correspondence is determined during DDS commissioning and checked during dosimetric and calibration procedures, as described in detail in Mirandola et al.⁷. Corrections for temperature and pressure are applied when the plan is converted.

Beam position at the isocentric plane vs strip chambers' reference system. To convert the positions at the isocentric plane reference system (in mm) to the chambers' one (in strip units), the divergence

170 of the beam, i.e. the beam angle after the scanning magnets, and measurements of the rotation and
 171 translation of the monitor chambers planes with respect to the isocentric plane were experimentally
 172 determined during DDS commissioning. Since the relation between the two reference systems could
 173 be affected by a tilt of the extracted beam, the correct position of the non-deflected pencil beam
 174 (nominal zero position) with respect to the isocenter is verified during daily QA, as reported in
 175 Mirandola et al⁷.

176 *Beam position at the isocentric plane vs currents for the scanning magnet power supplies.* For each
 177 of the two particle species, the beam position at the isocentric plane was measured during DDS
 178 commissioning, by varying the magnet current and the beam energy. The required parameters for the
 179 conversion were found through a fitting procedure. During daily QA the spot position is tested across
 180 the whole scanning area, according to the procedure described in Mirandola et al.⁷, and the test is
 181 passed if the deviation from the nominal position is within ± 1 mm. At the beginning of the clinical
 182 operations at CNAO, before the onset of the automatic position correction based on the feedback of
 183 the monitoring system, the correction of possible position offsets observed in the QA procedures was
 184 achieved by adding a constant position offset to this initial data conversion.

185 Position feedback correction

186 The beam position is reconstructed from the measurements of the BOX1 strip chambers using a center
 187 of gravity algorithm, when a minimum number of 100 counts is reached. This corresponds to 10^5 - 10^6
 188 protons, and to an average time of 4 ms (range 1-8 ms, according to the instantaneous beam intensity).
 189 The difference between the so obtained beam position and the prescribed one is continuously
 190 monitored by the DDS during the spot irradiation. Whenever such a difference exceeds a pre-defined
 191 threshold (2 mm), an interlock signal is issued, which immediately pauses the irradiation. As reported
 192 in Giordanengo et al.², the position interlock has to be manually reset by the operator for restarting
 193 the treatment. However, if the interlock persists the treatment has to be aborted. In summer 2013, i.e.
 194 few months after the patient treatments considered in this work, an online feedback correction of the

195 beam position was introduced to compensate for slow drifts of the beam position, presumably due to
196 the non-perfect dispersion at the isocenter and to small variations of the momentum along the spill.
197 Such small drifts sometimes lead to longer treatment times due to the occurrence of one or more beam
198 interlocks during the treatment. The method used is to convert the position difference into a current
199 offset value sent to the scanning system, which applies the correction. The applied correction at one
200 position is maintained as starting correction value for the next positions of the same beam energy and
201 same spill, where it can be updated. The current offset is reset when a new spill is generated.
202 Whenever the correction exceeds the threshold of 3 mm, an interlock signal is issued, which pauses
203 the irradiation. The spot position is measured twice: the first time to check the need of correction, and
204 eventually generate an interlock, the second time to calculate the position of the complete spot to be
205 reported in the log file. If the number of counts is below the minimum threshold required to
206 reconstruct the beam position with the center of gravity method, no feedback is applied and the spot
207 position of the strip with the largest number of counts is returned in the log file.

208 The described position correction approach is a self-correcting system, where the same detector used
209 for the position measurement (strip chambers) is also used for the correction. Such detector is not
210 placed at the isocenter. Therefore, the effectiveness of the correction method at the isocenter could
211 be evaluated through the QA checks of the spot position at the isocenter and across the scan field.
212 These QA checks are daily performed by the medical physics staff to verify the consistency between
213 the reference system (i.e. the isocenter) and the one of the strip chambers, using the all-in-one PTW
214 phantom loaded with strips of an EBT3 film for spot ⁷.

215 As already mentioned, to verify the correct position of the non-deflected pencil beam (nominal zero
216 position) with respect to the isocenter, a specific test is performed during daily QA. Moreover, the
217 accuracy of the pencil beam deflection by the scanning magnets across the whole scanning area is
218 independently checked through a spot pattern with nine beam spots in nominal positions (8 peripheral
219 and 1 central)⁷.

For 84% of the daily QA sessions in the period January 2012-July 2013, before the feedback implementation, the spot positions were within tolerance (± 1 mm) both in the center and at the edges of the scan field, for all particles, energies, and beam lines. For all the daily sessions considered, the mean absolute deviations (\pm rms) for the central position were 0.6 ± 0.4 mm in X and 0.4 ± 0.3 mm in Y, and 0.6 ± 1.0 mm in X and 0.4 ± 0.3 in Y for the edge positions. Ignoring the daily sessions which didn't pass the test and required the steering of the extraction lines before the patient treatment, the mean absolute deviations (\pm rms) for the central position were 0.5 ± 0.3 mm in X and 0.3 ± 0.2 mm in Y, and 0.4 ± 0.3 mm in X and 0.3 ± 0.2 in Y for the edge positions. The same analysis performed in the period July 2017-November 2018, after feedback implementation, showed an increase in the percentage (94%) of the daily QA sessions with spot positions within tolerance (± 1 mm) both in the center and at the edge positions. For all the daily sessions considered, the mean absolute deviations (\pm rms) for the central position were 0.5 ± 0.3 mm in X and 0.5 ± 0.4 mm in Y, and 0.5 ± 0.3 mm in X and 0.5 ± 0.4 in Y for the edge positions. The same analysis, ignoring the daily sessions which didn't pass the QA test, results in a mean absolute deviation (\pm rms) of 0.4 ± 0.3 mm in X and 0.4 ± 0.3 mm in Y for the central position, and 0.4 ± 0.3 mm in X and 0.5 ± 0.3 in Y for the edge positions.

Correction of delivered particle numbers in the log files

The treatment log file, provided by the DDS at the end of each treatment, is based on the DDS raw data stored during the field delivery.

The analysis performed for this work used log files and raw data of the DDS produced during the initial clinical activity. More specifically, the raw data saved by the DDS at the end of each spill are used to correct for the two following systematic effects, inherent in the data saved in the log files. It should be observed that later versions of the DDS are implementing such corrections when the log files are produced.

- 1) The system is designed so that whenever one of the two large-area parallel plate ionization chambers reaches the prescribed number of counts specified by the TPS, the delivery of the spot is terminated and the sequence is moved to the following spot. For the second chamber, used for redundancy and as a safety monitor, the prescribed number of counts is increased by 10% to let the first chamber alone trigger the end of the spot. It may be observed that, although very rarely and only at little requested counts, the second chamber can reach the prescription before the first chamber because of negative dark current effects in the first chamber, leading to a wrong count of particles. The information on which of the two large-area parallel plate chambers reached the prescribed dose is recorded in DDS raw data on a spot-by-spot basis, but the log file uses the data of the first chamber, so a correction was applied to account for this effect in the calculation of the number of particles delivered.
- 2) Because of noise and background current, mainly due to the leakage currents of the large-area parallel plate chambers, some counts are measured even without the beam, during the inter-spill time. These counts, either positive or negative, affect the dose delivered to the first spot of each spill, as they are added to the actual number of counts for that spot. Since the information about the dark counts measured in the inter-spill time is available in the raw data, it has been used to correct under- or over-counting of first spots on the log files.

Analysis of the treatment fields

3837 fields from all the 62 patients consecutively treated with protons and carbon ions between January 2012 and April 2013 have been analyzed. The range of values for the main delivery parameters is listed in Table 1.

265 **Table 1. Analyzed Fields Statistics. Pat. = patient**

	N. patients	Total n. of fields	Fields/pat. (min-max)	Slices/pat. (min-max)	Spots/slice (min-max)	Prescribed particles/pat. (min-max)	Energy (min-max) [MeV/u]
proton	46	3411	15 - 147	848–9419	1–1145	4.85E+11–1.37E+13	62–227
carbon	16	426	4 - 60	120–2733	1–4628	1.27E+09 –2.06E+11	115–399

266

267 As a first step of this analysis, the accuracy of the DDS has been investigated by comparing for each
 268 field both the positions of spots at the isocentric plane, determined from the strip chambers as
 269 previously described, and the number of particles per spot measured by the DDS with the
 270 corresponding prescriptions from the TPS. The analysis has been performed separately for treatments
 271 delivered in room 1 and 3 and for protons and carbon ions in order to isolate possible systematic
 272 effects due to the particle type or to the beam line and DDS. Room 2 has been commissioned in late
 273 September 2013 and therefore wasn't considered in this study.

274 Secondly, these quantities have been used to create two 3D physical dose maps, one for the
 275 prescription and one for measured data, by using a validated dose computation software¹². The
 276 correspondence of the two dose distributions has been evaluated with the gamma-index method using
 277 a 2 mm grid spacing with 0.2 mm resolution, 2 mm Distance-To-Agreement (DTA) and 2% Dose
 278 difference¹³.

279 The analysis of the maximum gamma value and of the percentage of points with $\gamma \leq 1$ (*passing*
 280 *volume*, in the following) was performed as a function of the day of the treatment. More specifically,
 281 the analysis was performed separately for the two sets of daily fractions, which characterize the course

282 of the treatments analyzed: the first series of fractions (called *1st Phase*) and the second set (called
283 *Boost*) delivered in the last days of treatment.

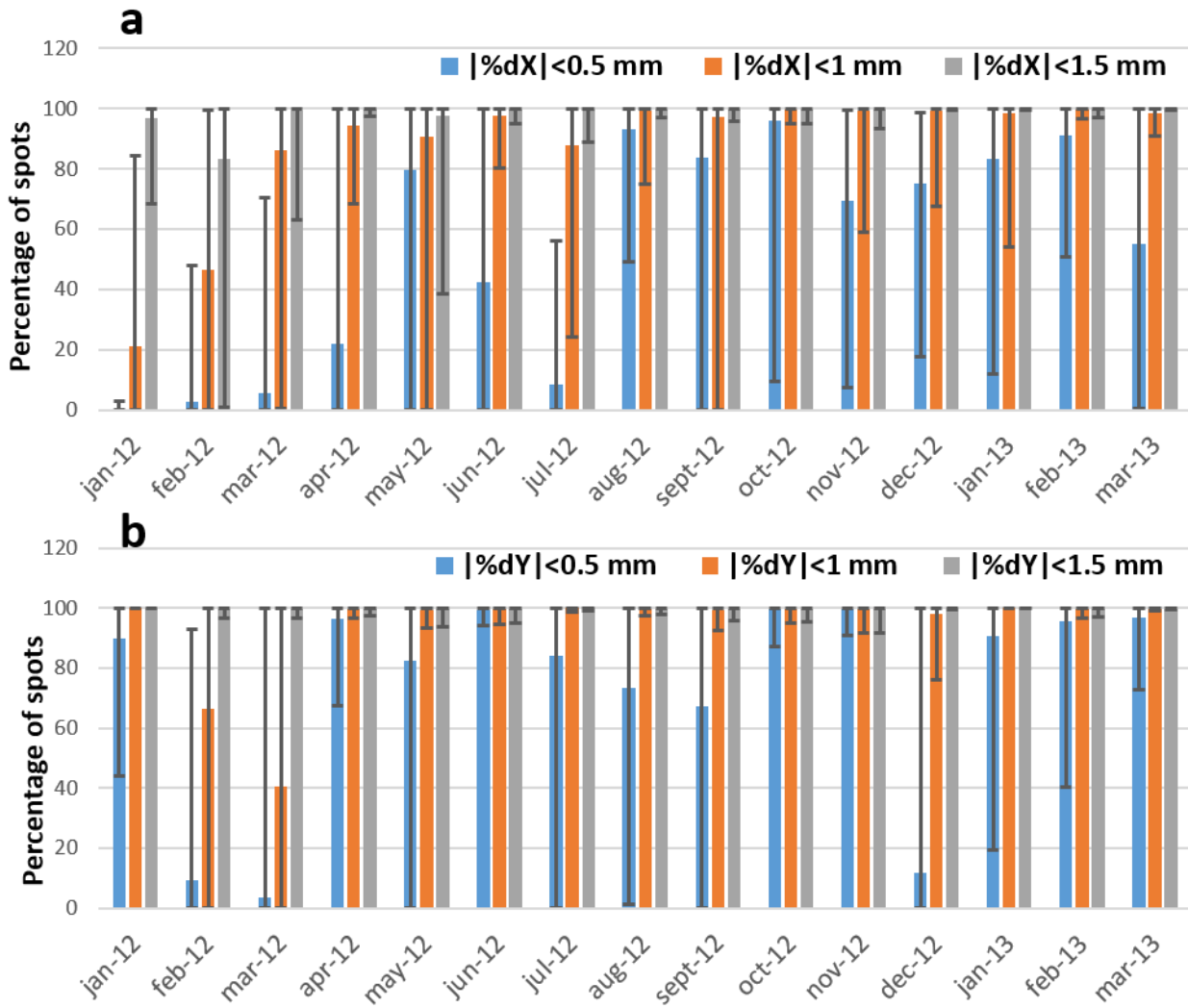
284 In both cases, the maximum gamma value and the *passing volume* for each individual field and for
285 the sum of the different fields delivered in the same day were reported. In parallel, the correlation
286 between the deviations observed in the measured number of particles or spot positions and the
287 accuracy of delivered dose has been looked at.

288 As an example, the 3D maps comparison of prescribed and delivered dose is reported for a patient
289 affected by chordoma of the skull base treated in room 1 (protons) with a total of 37 fractions. This
290 patient was selected because representative of a treatment with deviations between prescribed and
291 delivered dose distributions. The aim is twofold: to verify the effect of the spot position accuracy on
292 the dose distribution and to study the impact of the online feedback correction of spot position
293 deviations described earlier. For the latter study, the same treatment was repeated on a PMMA block,
294 and the dose comparison was performed with the acquired data.

295 **Results**

296 Spot position accuracy

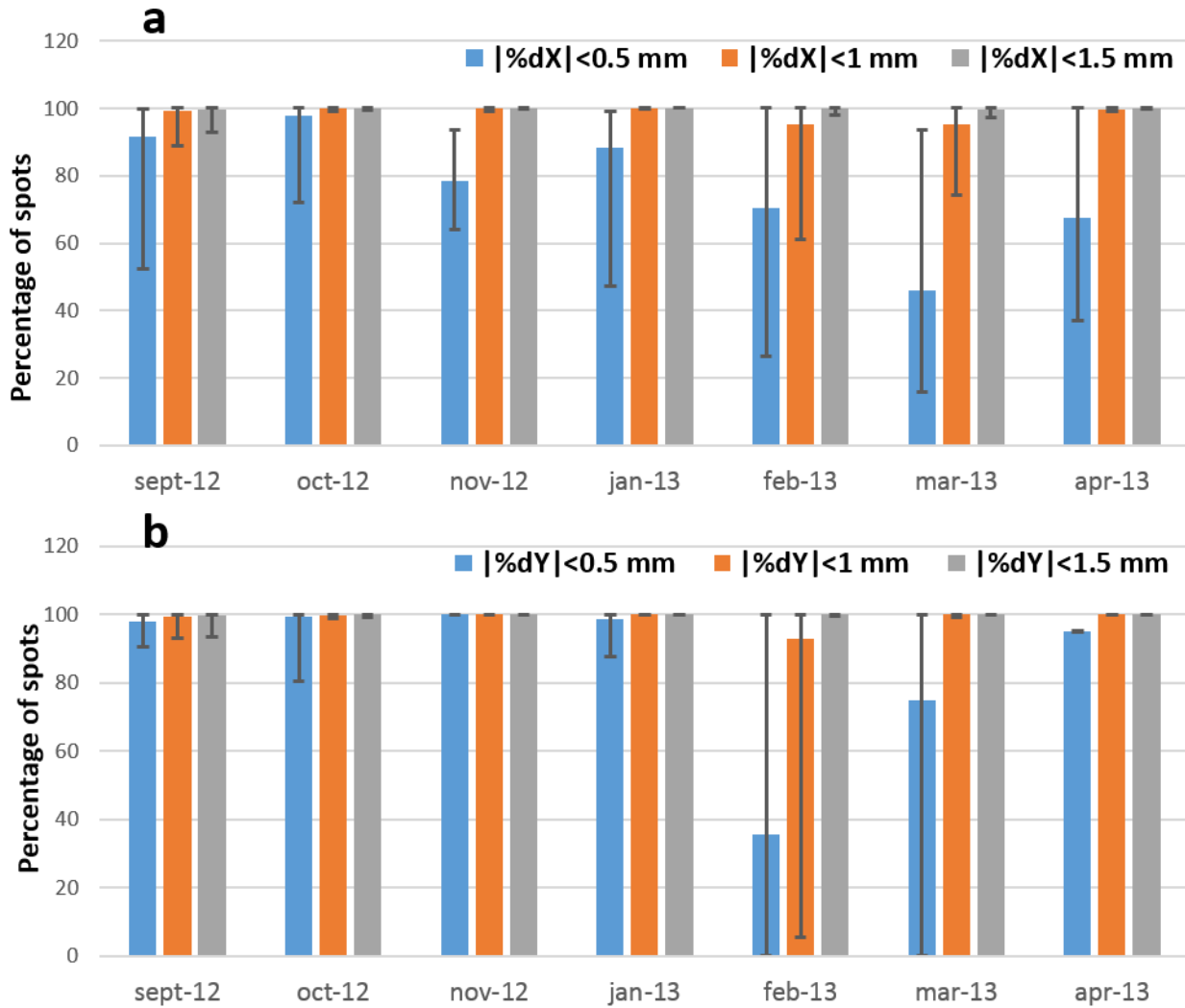
297 The absolute difference between the measured and prescribed spot positions at the isocentric plane
298 have been studied separately in the horizontal (X) and vertical (Y) directions. The fraction of spots
299 with such a difference within three different thresholds (0.5, 1, and 1.5 mm) has been calculated for
300 each field irradiated between January 2012 and April 2013 in room 1 (protons) and 3 (protons and
301 carbon ions). The results have been grouped per month of delivery and reported in Fig. 1, 2 and 3.



302

303 *Figure 1. Mean value of the percentage of spots whose position differs from the prescription less than 0.5*
 304 *mm (blue bars), 1 mm (orange bars), 1.5 mm (gray bars), for all fields treated with protons in room1, along*

305 *X direction (a) and Y direction (b). The minimum and maximum percentage values of the fields irradiated*
 306 *in each considered month are displayed as solid vertical bars for the three different thresholds.*



307

308 *Figure 2: Mean value of the fraction of spots whose position differs from the prescription less than 0.5 mm*
 309 *(blue bars), 1 mm (orange bars), 1.5 mm (gray bars), for all fields treated with protons in room3, along X*
 310 *direction (a) and Y direction (b). The minimum and maximum percentage values of the fields irradiated in*
 311 *each considered month are displayed as solid vertical bars for the three different thresholds.*

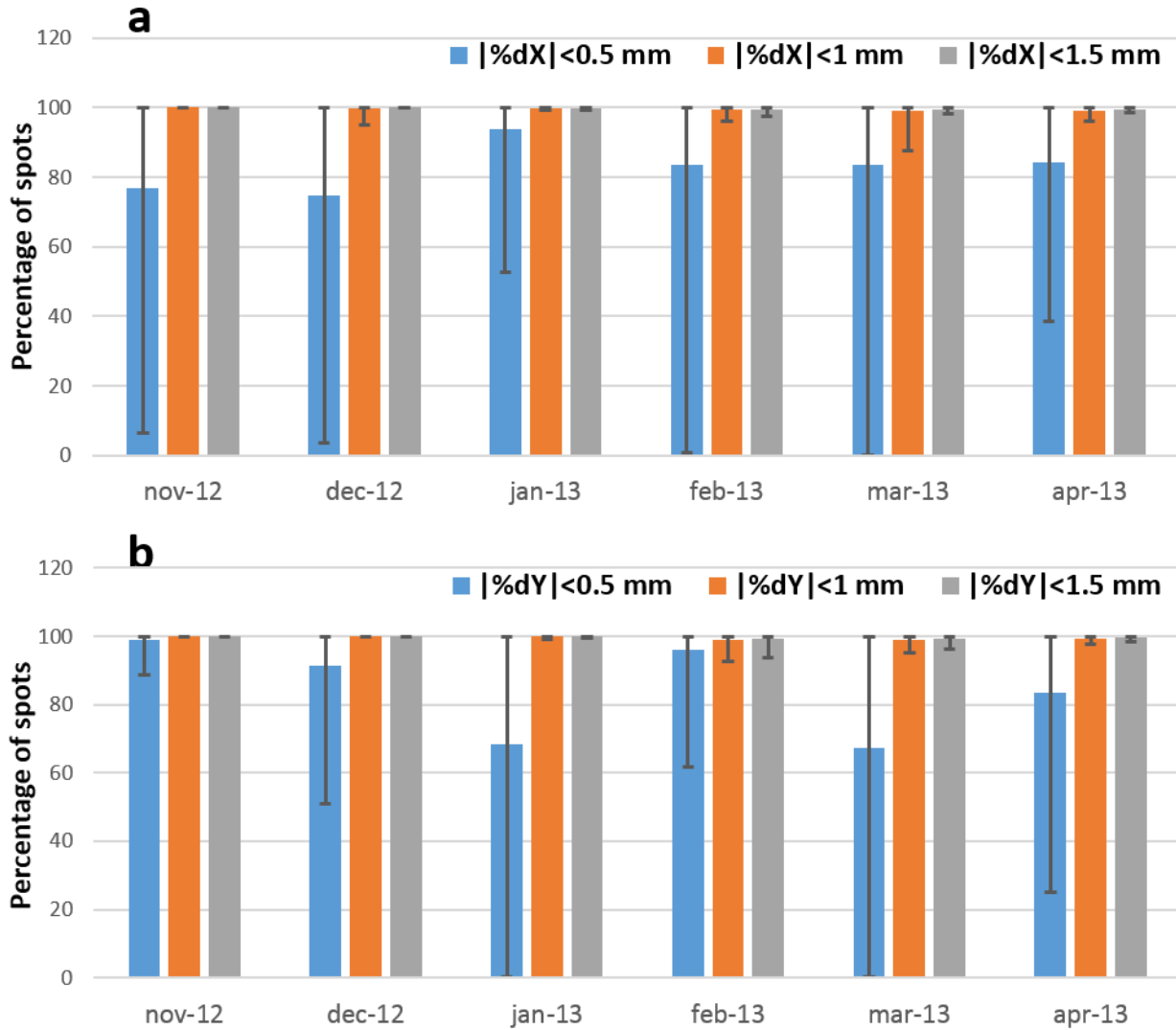
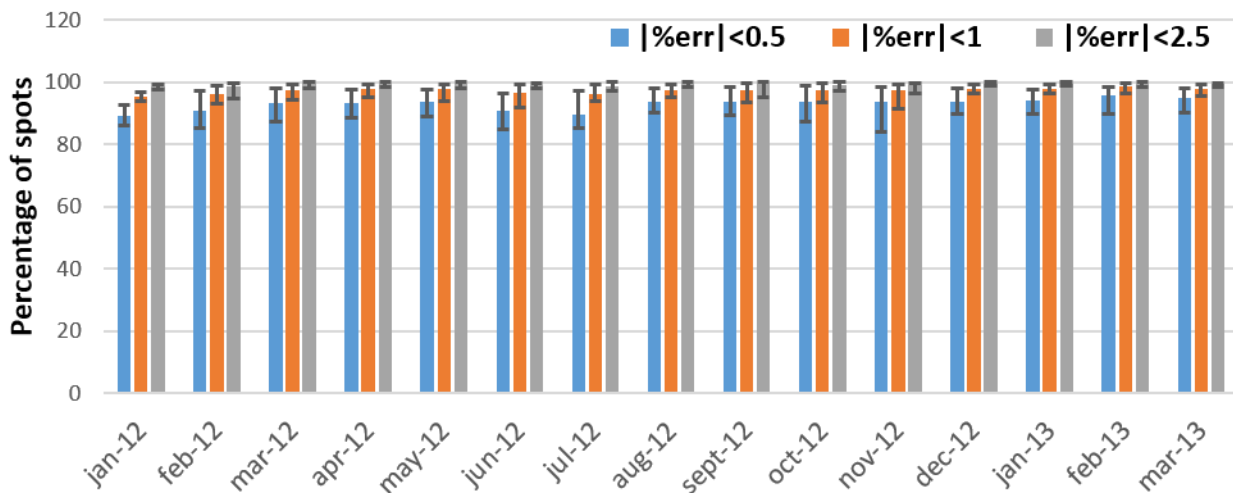


Figure 3: Mean value of the fraction of spots whose position differs from the prescription less than 0.5 mm (blue bars), 1 mm (orange bars), 1.5 mm (gray bars), for all fields treated with carbon ions in room 3, along X direction (a) and Y direction (b). The minimum and maximum percentage values of the fields irradiated in each considered month are displayed as solid vertical bars for the three different thresholds.

Fig. 1, 2 and 3 show a better spot positioning stability in Y compared to X direction. This can be explained by the more complex beam dynamics in the horizontal plane, where the acceleration and the beam extraction occurs. It can also be noticed that few small tunings of the accelerator optics were necessary to realign the beam vertically in room 1. Indeed, as explained in Mirandola et al.⁷, beam steering adjustments were performed when the beam optics was causing the results of daily checks to deviate more than twice the tolerance level or to remain out of tolerance for two consecutive days.

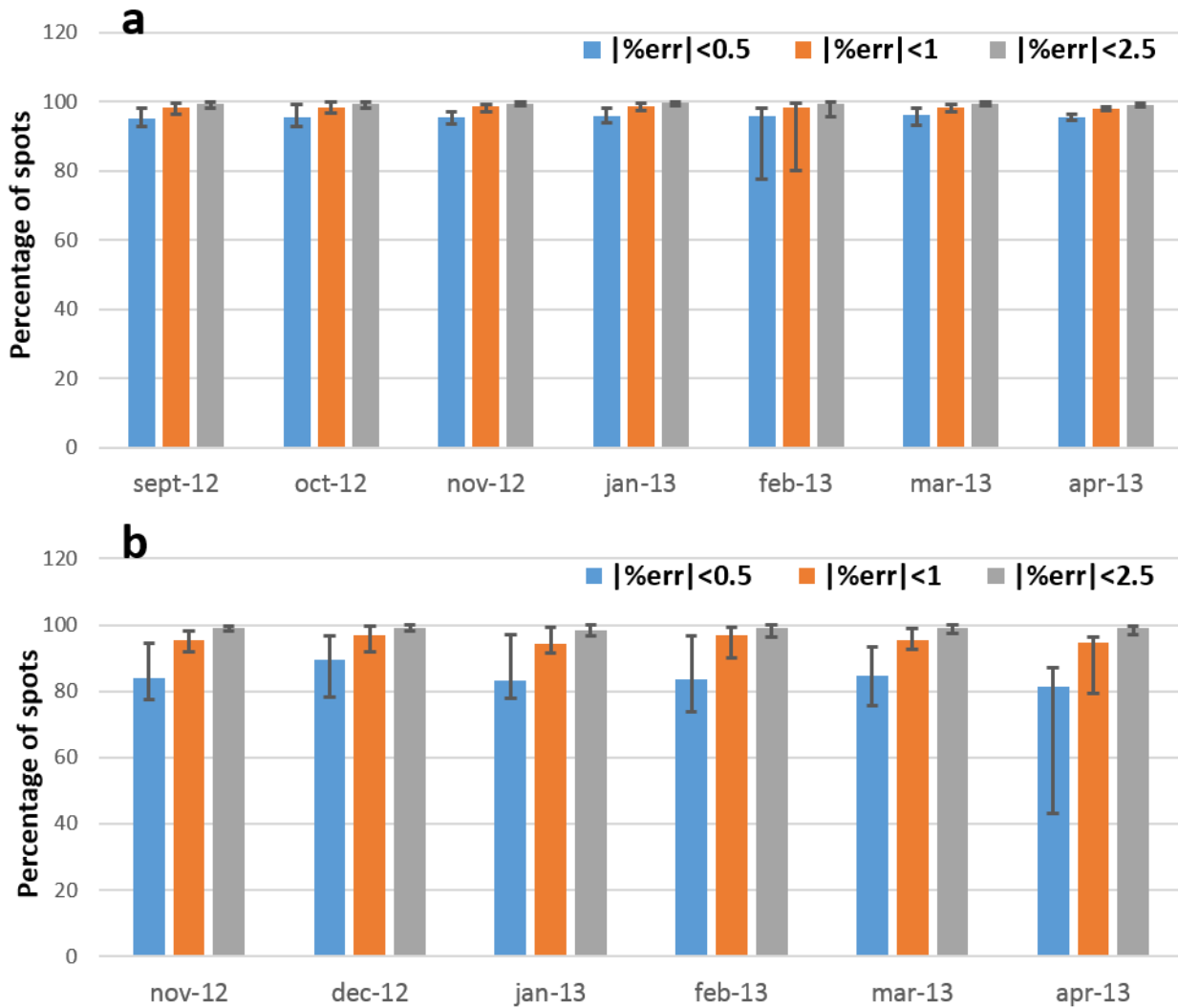
323 Accuracy of the number of particles delivered

324 The relative difference between the number of prescribed and delivered particles per spot was studied,
 325 and the percentage of spots with relative difference within three thresholds has been calculated for
 326 each irradiated field and is reported as function of treatment month in Fig. 4 for proton treatments in
 327 room 1, in Fig. 5a for proton treatments in room3 and in Fig. 5b for carbon ion treatments in room 3.



328

329 **Figure 4: Mean value of the percentage of spots with relative difference between prescribed and delivered**
 330 **number of particles within three different tolerances: 0.5% (blue bars), 1% (orange bars), and 2.5% (gray**
 331 **bars) for all fields treated with protons in room 1. The minimum and maximum percentage values of the**
 332 **fields irradiated in each considered month are displayed as solid vertical bars for the three different**
 333 **thresholds.**



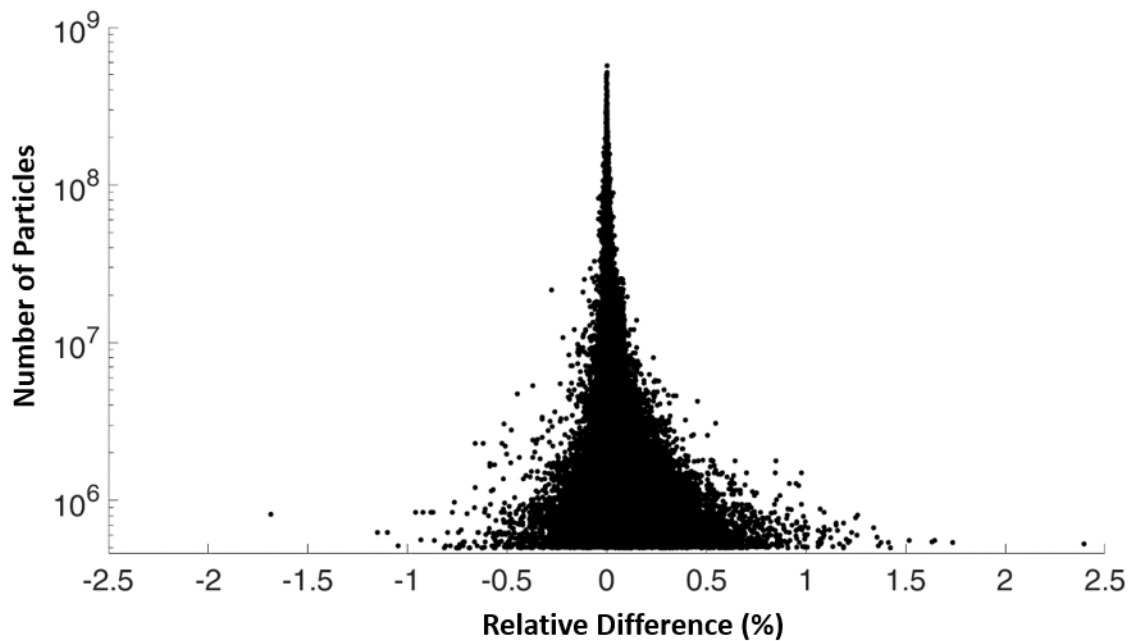
334

335 **Figure 5. Mean value of the percentage of spots with relative difference between prescribed and delivered**
 336 **number of particles within three different tolerances: 0.5% (blue bars), 1% (orange bars), and 2.5% (gray**
 337 **bars) for all fields treated with protons (a) and carbon ions (b) in room 3. The minimum and maximum**
 338 **percentage values of the fields irradiated in each considered month are displayed as solid vertical bars for**
 339 **the three different thresholds.**

340 Significant daily fluctuations are not observed in the deviations in number of particles: 98% of spots
 341 falls within the 2.5% difference, while 94-96% of spots falls within 1.0% difference.

342 The highest precision threshold of 0.5% results in larger fluctuations: 85-95% of spots in room 1, 91-
 343 97% in room 3 for treatments with protons and 75-96% for treatments with carbon ions.

344 The deviations in the number of particles are dominated by the error on the quantization in the
 345 conversion from monitor counts to particles, as one charge quantum corresponds to about 10^4 protons
 346 and to about 500 carbon ions. The relative effect of the quantization depends on the number of
 347 particles prescribed in the spot. Since the transversal scanning step used in the CNAO clinical practice
 348 is 2 mm for carbon ions and 3 mm for protons, the dose (i.e. the number of particles) per spot is on
 349 average lower for carbon ions, in respect to protons. Moreover, the increased relative biological
 350 effectiveness of carbon ions further reduces the dose required (i.e. the number of particles) per spot
 351 for carbon treatments, with respect to proton treatments¹⁶. As a result, an increased relative error due
 352 to the quantization explains the larger fluctuations in the deviations of the number of particles for
 353 carbon treatments. Moreover, Fig. 6 shows that the larger relative fluctuations are measured, as
 354 expected, for spots with smaller number of particles, and thus reduced clinical relevance.



355

356 *Figure 6. Distribution of the prescribed particles for each spot as a function of the percentage relative*
 357 *difference between prescribed and delivered number of particles ($\Delta\text{particles}/\text{particles}$) for room 1 (protons).*

358 Impact on delivered dose distributions

359 Neither the deviations in beam positions nor the ones in number of particles provide any direct
360 information regarding their impact on the delivered dose to the patient, which represents the relevant
361 quantity to evaluate the quality of the treatment. Therefore, both the planned and the measured
362 number of particles and spot positions have been used as input of a dose reconstruction engine of a
363 TPS software¹² to calculate and compare the delivered and the planned physical dose distributions in
364 patient anatomy.

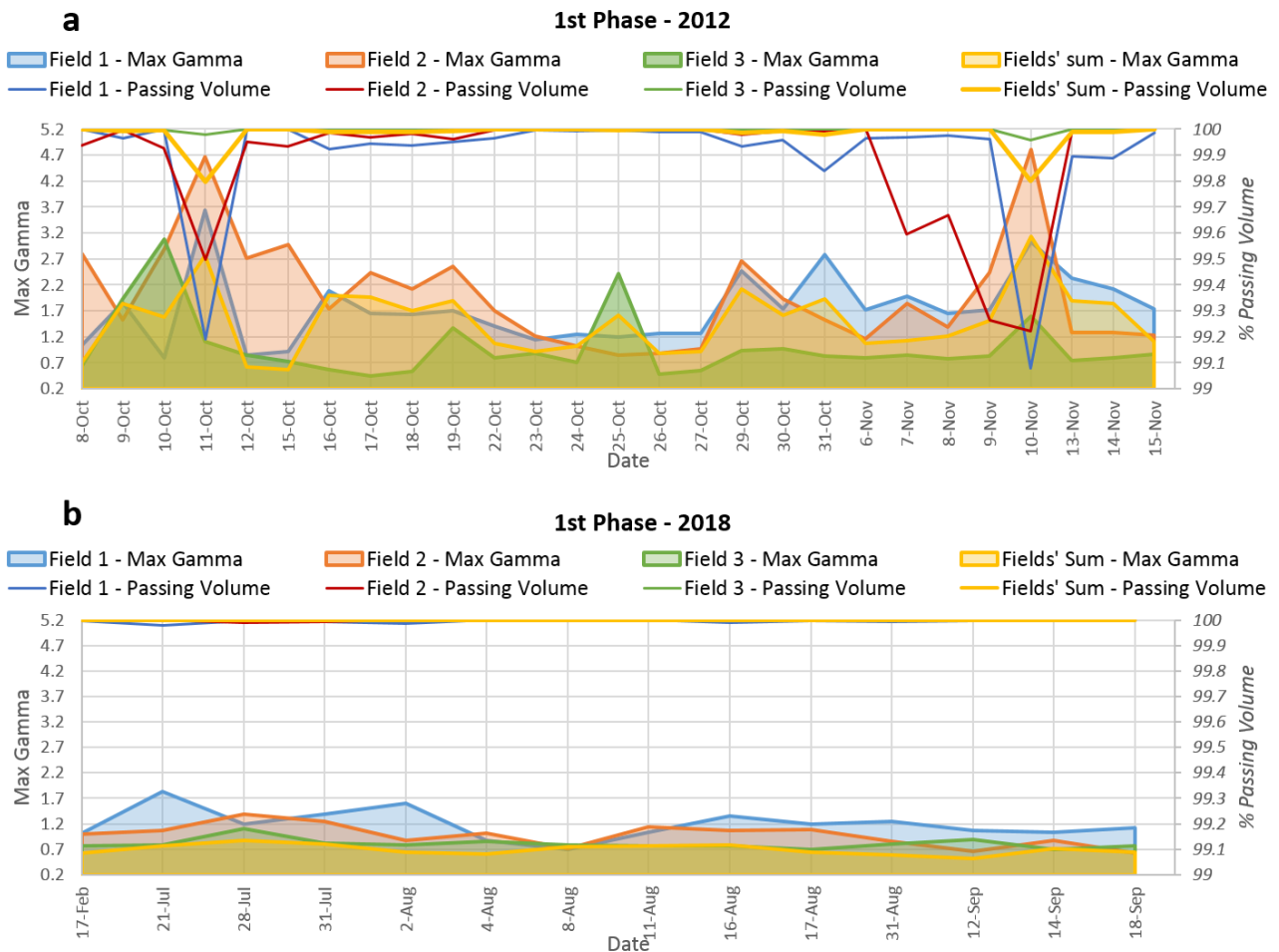
365 The prescribed dose maps and the delivered ones were compared for several patients, showing on
366 average negligible discrepancies (*passing volume* percentage larger than 99.8% for the sum of all
367 fields) for both protons and carbon ions treatments. It should be emphasized that such an analysis
368 relies on the number of particles and positions at the strip chambers' reference system. Thus, possible
369 deviations at the isocenter could be possible, although within the clinically accepted tolerances, as
370 verified by the daily QA checks described at the end of the previous section *position feedback*
371 *correction*.

372 For the sake of concision and clarity, one case study will be reported in the following, chosen because
373 of noteworthy values of gamma index and passing volume percentage for some fractions.

374 This patient was diagnosed with chordoma of the skull base, with infiltration of the cavernous sinus,
375 treated in room1 between October and December 2012 (protons). Daily dose of 2 Gy (RBE) was
376 given to the tumor target for a total dose of 74 Gy (RBE) in 37 fractions (27 fractions *1st Phase* and
377 remaining 10 as *Boost*). Both *1st Phase* and *Boost* fractions are composed by three fields. The gamma
378 matrix was calculated for all fields.

379 For this case, both the *1st Phase* and *Boost* fields were re-delivered several times in 2018 on a PMMA
380 block to collect statistic data and evaluate the improvement in delivery uncertainties with respect to
381 2012, which can be mainly ascribed to the implementation of the position correction feedback loop.

Fig. 7 shows the maximum value of gamma-index among all the voxels and the *passing volume* percentage, i.e. the fraction of voxels with gamma value lower than 1, for each field and for the sum of the three *1st Phase* fields, both for delivered treatment in 2012 (Fig. 7a) and in 2018 (Fig. 7b). Figure 8 shows the same quantities for the *Boost* fields.



386

Figure 7: *1st Phase* max gamma (area graphs) and percentage of voxels with gamma value lower than 1 (line graphs) for the treatment of one example patient (protons) delivered in 2012 (a) and re-irradiation in 2018 (b).

389

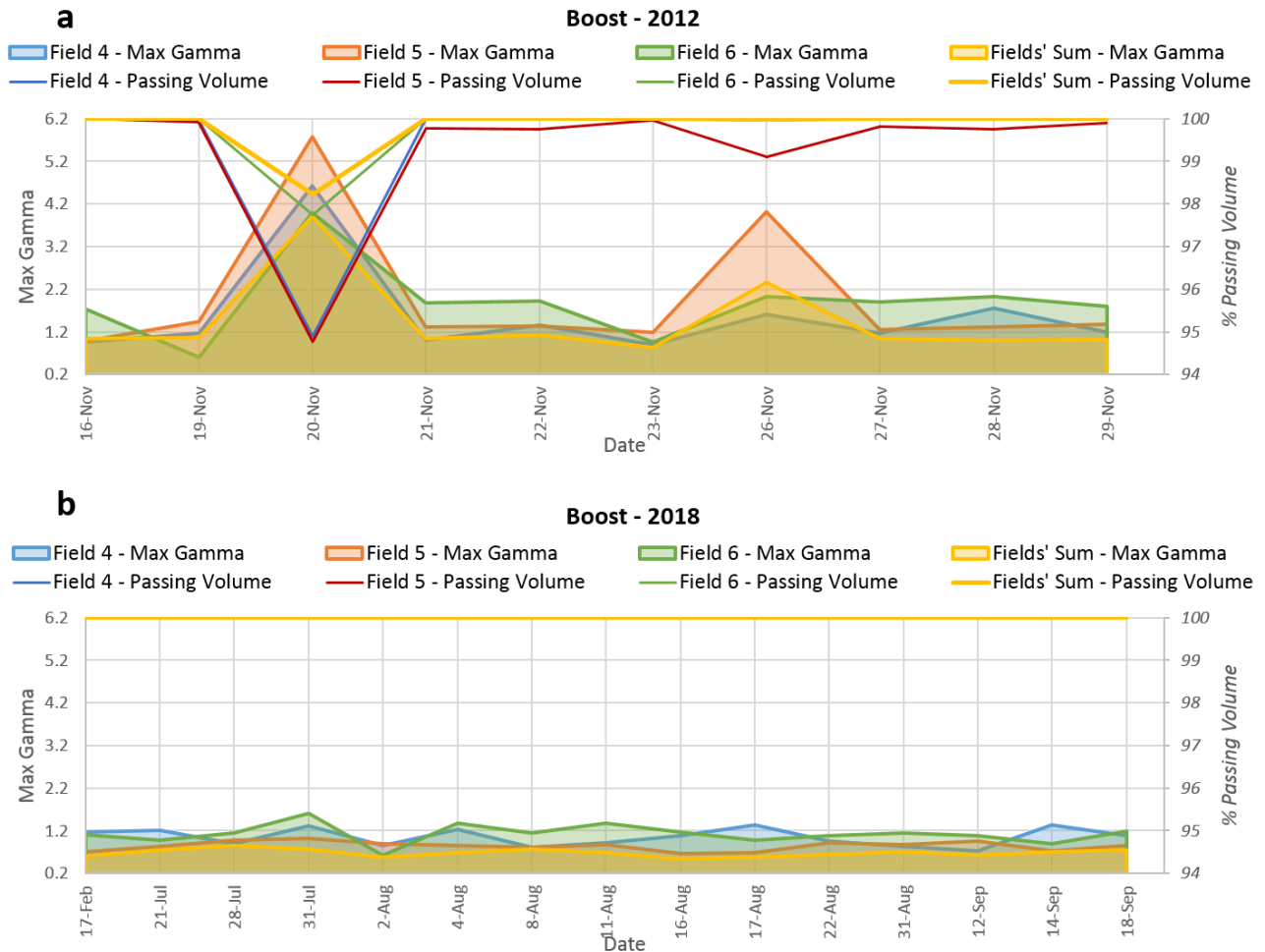


Figure 8. Boost max gamma (area graphs) and percentage of voxels with gamma value lower than 1 (line graphs) for the treatment of one example patient (protons) delivered in 2012 (a) and in 2018 (b).

Maximum values of gamma-index for 1st Phase fractions irradiated in 2012 are almost always larger than one both for each field (up to a value of 4.8 on November 10 for Field 2) and for the sum of all fields (up to a value of 3.1 on November 10). However, the passing volume percentage is 99.1% in the worst case (Field 1 on November 10) and, what is more important from a clinical point of view, it is always larger than 99.8% for the sum of all fields. This suggests that dose discrepancies are localized in a limited number of voxels. Indeed, the thorough analysis of the 3D distribution of gamma shows that those large values are connected to isolated voxels in regions of low dose and/or high dose gradients, as shown by the isocurves plot in Fig. 9. The clinical relevance of these discrepancies would require the analysis of the volumes at risks, which is out of the scope of the present work.

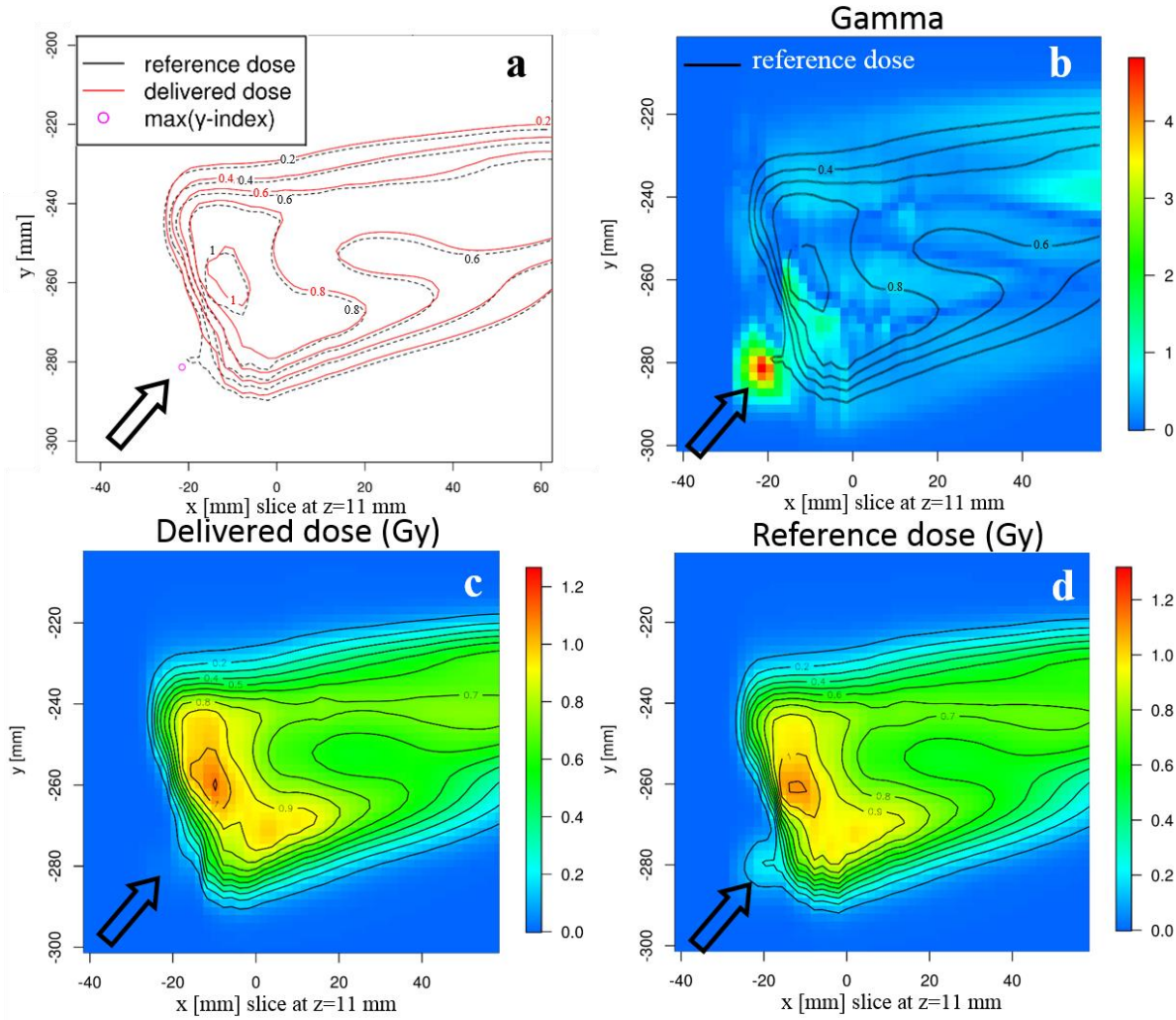


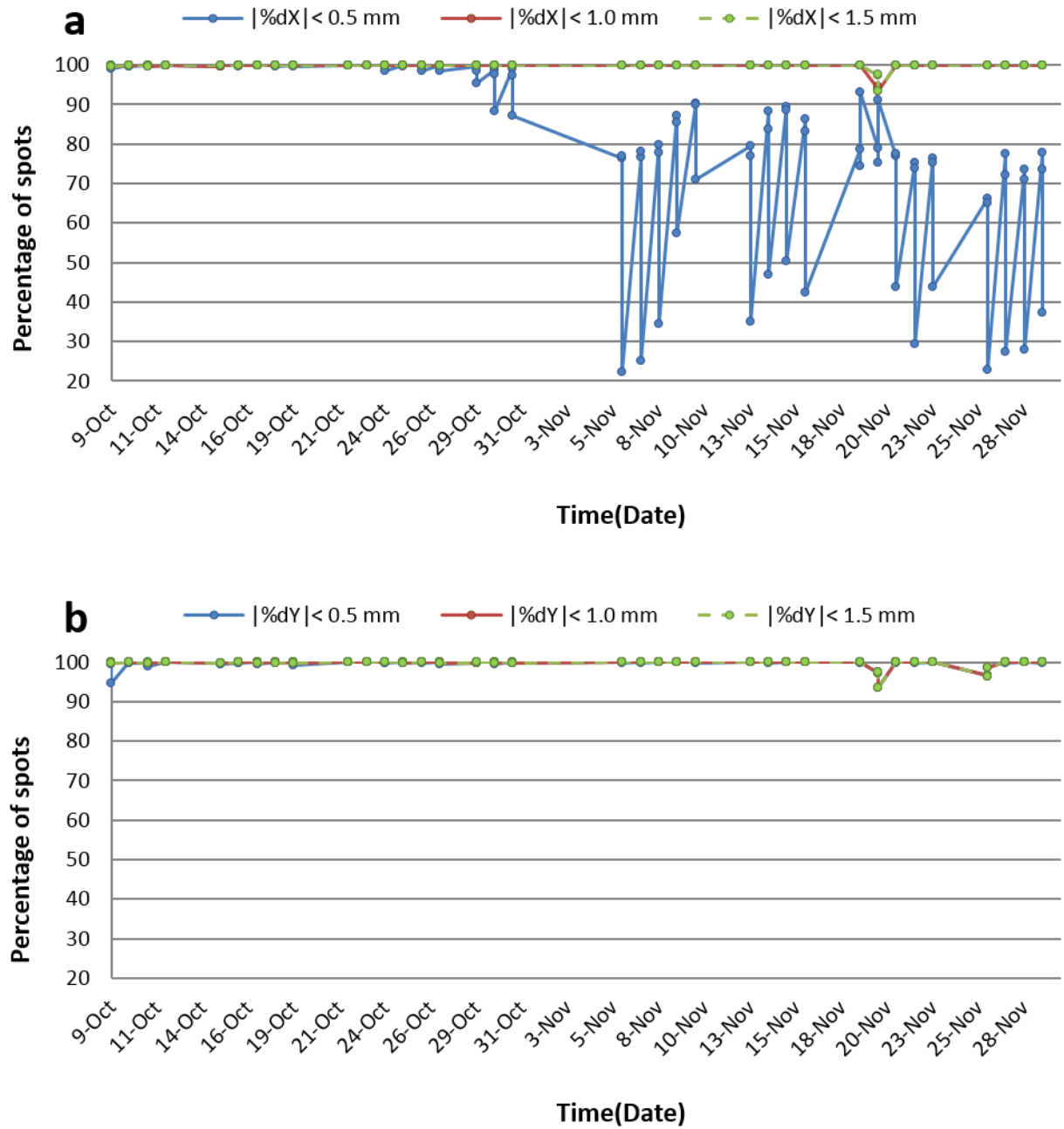
Figure 9. Isodose curves (a), gamma-index distribution (b), delivered dose (c) and reference dose (d) for the plane x - y at a specific z ($z=11$ mm) in the CT reference system, for one field. The black arrows points at the pixel corresponding to the maximum gamma value.

On the contrary, the same 1^{st} Phase fields re-irradiated in 2018 (Fig. 7b) show a maximum value of gamma-index always lower than 1 for the sum of the three fields, reaching 1.8 as worst value for Field 1 on July 21. As before, gamma values larger than 1 are referable to a few single voxels, given the passing rate constantly above 99.99%.

Comparing Fig. 7a and 7b, the feedback correction on spot positions seems to improve the day-by-day stability of the delivered dose, leading to an overall better correspondence. However, the improvements are affecting only a limited fraction ($\sim 0.2\%$) of the voxels of the irradiated region

413 where high dose gradients occur. Considering the magnitude of the dose uncertainties related to
414 patient positioning, changes in patient morphology and moving organs, the improvement in spot
415 position accuracy does not seem to be clinically relevant.

416 Similar conclusions can be drawn by comparing the *Boost* fractions in Fig. 8. Maximum values of
417 gamma-index for the sum of *Boost* fractions irradiated in 2012 are equal or smaller than 1 for each
418 day of delivery, with the exception of November 20, where the maximum gamma values are 3.9. For
419 all treatment days, the passing rate is almost 100% for the sum of the *Boost* fields, while that
420 percentage drops to 98.2% on November 20. The reason for it is related to an instability, occurring
421 on November 20, of an element of the accelerating system, which led to the observed systematic
422 deviation. Indeed, the graphs of spot position deviations as a function of *Boost* treatment days (Fig.
423 10) are in agreement with the high variability observed for the < 0.5 mm threshold in X and Y in the
424 considered period (January 2012 – April 2013), while a reduction of 6% is shown for the fraction of
425 spots within 1.0 and, especially, 1.5 mm tolerance at that date.



426

427 *Figure 10. Fraction of spots whose position in X (a) and in Y (b) differs from the prescription by less than*
 428 *0.5 mm (blue markers), 1 mm (red markers), 1.5 mm (green markers), for the three Boost fields of the case*
 429 *study under consideration.*

430 Discussions

431 The first aim of the present work was to fill up the lack of a detailed retrospective analysis of the DDS
 432 performances in the initial period of CNAO clinical activity.

433 As expected by the very nature of the DDS, which reproducibly works independently of the
434 accelerator, the number of particles was found to be stable. Indeed, the deviations in the number of
435 particles originate from the quantization error in the conversion from monitor counts to particles.

436 On the contrary, the analysis showed systematic deviations of spot positions within 0.5 mm for only
437 part of the fractions delivered. However, with the exception of the first two months of operation of
438 room 1, deviations were always within 1.5 mm and almost always within 1 mm.

439 The observed deviations in specific periods were caused by beam lateral offsets and were accurately
440 monitored by the QA measurements daily performed at the isocenter. In order to compensate for this
441 effect and to achieve a precise delivery of the dose to the patient, a constant position offset was added
442 to the initial data conversion from the beam position at the isocentric plane to the currents for the
443 scanning magnet power supplies, to ensure that deviations of the spot positions at the isocentric plane
444 were always within ± 1 mm. These constants were obtained by averaging the corrections over all the
445 beam energy range and were updated daily based on the result of the QA checks performed
446 overnight⁷. If deviations larger than 1 mm for individual energy values were still observed after
447 correction, a complete beam steering correction intervention was immediately requested by medical
448 physicists to accelerator physicists. Excluding cases where deviations larger than 1.5-2 mm were
449 found, the updated steering setting was determined as soon as daily clinical activity was terminated
450 and applied the next day.

451 To reduce the time for an irradiation and correct for beam position deviations without stopping the
452 irradiation, charged particle facilities have adopted different methods, such as dead reckoning via the
453 algorithmic tables or formulas, beam tuning on the first energy layer, adaptive beam tuning with
454 application of the position offset corrected in the first energy layer to all subsequent layers, and
455 adaptive scanning magnet correction with beam position correction within a scan¹⁷. The latter has
456 been chosen by CNAO as feedback loop approach, and it is also used by other facilities, such as
457 GSI^{18–20}, HIT and HIMAC²¹.

458 To complete the investigation of the lateral deviation of the pencil beam during scanning, this work
459 also considers the improvements made by the introduction of the feedback algorithm for the
460 correction of small position deviations, in terms of impact on dose distributions. The implementation
461 of the latter algorithm in the DDS allowed reducing the occurrence of beam interlocks during the
462 treatment, improving the day-by-day DDS stability.

463 The aim of this study is to verify the efficiency of the beam scanning system in reproducing the
464 expected spot position and number of particles at the location of the monitoring chambers and to
465 quantify the improvement that has been achieved by the introduction of feedback correction,
466 evaluated in terms of gamma-index. It is worth noticing that evaluating the global performance of the
467 DDS would require an independent measurement of spot position and number of particles at the
468 isocenter. This is out of the scope of the present work, and has been reported in the work of Mirandola
469 et al.⁷, where the DDS commissioning and the daily QA results and procedures are extensively
470 described.

471 In order to evaluate the impact of spot position and particle deviations on dose distributions, and the
472 effect of the feedback correction, a representative case was reported. The case consists of a patient
473 treated with protons in 2012, whose treatment was repeated on a PMMA block, in 2018.

474 A dose calculation tool was fed with the measured number of particles and spot positions from the
475 log files; planned and delivered dose distributions were compared, before and after feedback
476 implementation, through gamma-index calculation.

477 The variability of the maximum gamma for the real irradiation (2012) was found to be higher than
478 that of the same treatment delivered in 2018. However, the 2012 *passing volume* was found to be
479 larger than 99.8% for the sum of all fields, which is comparable to the 2018's value, with the
480 exception of one day with 98.2% passing volume, probably related to an instability of the accelerating
481 system.

482 It is worth noting that the clinical effect of the variability found in the maximum gamma for the 2012
483 irradiation is mitigated by averaging along the number of fractions, and the high percentage of *passing*
484 *volumes* confirmed the accuracy of the delivery. However, it is equally interesting to consider that in
485 principle the introduction of a position feedback and the increased beam control capability acquired
486 after the first years of clinical experience led to an evident improvement both in the DDS stability,
487 evaluated in terms of gamma index as measure of the impact on dose distributions, and in the stability
488 of operation by reducing the number of interlocks.

489 **Conclusions**

490 The retrospective analysis of the DDS accuracy during the initial clinical activity at CNAO was
491 described, its impact on dose maps was studied, and the effect of the implementation of a position
492 feedback algorithm on the dose distribution was evaluated. No deviation worthy of interest was found
493 between the number of particles prescribed by the TPS and measured by the DDS, while the
494 deviations found in the spot positions should be mainly ascribed to daily fluctuations and accelerator
495 tuning. The introduction of the position feedback, together with the increased beam control capability
496 acquired after the first year of clinical experience, was evaluated in terms of gamma-index of 3D dose
497 maps (prescribed versus delivered) before and after feedback implementation. Although the effect of
498 deviations, and therefore the improvement due to the feedback algorithm, was found to be of moderate
499 clinical impact in terms of dose delivery accuracy, it is worth acknowledging that the introduction of
500 the position feedback increased the stability of operation and minimized the treatment duration by
501 reducing the occurring interlocks.

502 **Acknowledgements**

503 The authors thank Dr. Marco Pullia for his help while writing the paper.

504 **Disclosure of Conflicts of Interest**

505 The authors have no relevant conflicts of interest to disclose

506 **REFERENCES**

- 507 1. Jäkel O. Treatment Planning for Ion Beam Therapy. In: Ute Linz, ed. *Ion Beam Therapy.*
508 *Fundamentals, Technology, Clinical Applications.* Springer, Berlin, Heidelberg; 2012:503-
509 525. doi:10.1007/978-3-642-21414-1_30
- 510 2. Giordanengo S, Garella MA, Marchetto F, et al. The CNAO dose delivery system for
511 modulated scanning ion beam radiotherapy. *Med Phys.* 2015;42(1):263-275.
512 doi:10.1118/1.4903276
- 513 3. Orecchia R, Vitolo V, Fiore MR, et al. Proton beam radiotherapy: report of the first ten patients
514 treated at the “Centro Nazionale di Adroterapia Oncologica (CNAO)” for skull base and spine
515 tumours. *Radiol Med.* 2014;119(4):277-282. doi:10.1007/s11547-013-0345-0
- 516 4. Molinelli S, Mairani A, Mirandola A, et al. Dosimetric accuracy assessment of a treatment
517 plan verification system for scanned proton beam radiotherapy: one-year experimental results
518 and Monte Carlo analysis of the involved uncertainties. *Phys Med Biol.* 2013;58(11):3837-
519 3847. doi:10.1088/0031-9155/58/11/3837
- 520 5. Lomax A. Physics of Treatment Planning Using Scanned Beams. In: Paganetti H, ed. *Proton*
521 *Therapy Physics.* CRC Press; 2018:483-518.
- 522 6. Yeung DK, Palta JR. Precision and uncertainties in Planning and Delivery. In: Paganetti H, ed.
523 *Proton Therapy Physics.* CRC Press; 2018:519-550.
- 524 7. Mirandola A, Molinelli S, Vilches Freixas G, et al. Dosimetric commissioning and quality
525 assurance of scanned ion beams at the Italian National Center for Oncological Hadrontherapy.
526 *Med Phys.* 2015;42(9):5287-5300. doi:10.1118/1.4928397
- 527 8. Coutrakon G, Wang N, Miller DW, Yang Y. Dose error analysis for a scanned proton beam
528 delivery system. *Phys Med Biol.* 2010;55(23):7081-7096. doi:10.1088/0031-9155/55/23/S09

- 529 9. Giordanengo S, Manganaro L, Vignati A. Review of technologies and procedures of clinical
530 dosimetry for scanned ion beam radiotherapy. *Phys Medica*. 2017;43:79-99.
531 doi:10.1016/j.ejmp.2017.10.013
- 532 10. Scandurra D, Albertini F, van der Meer R, et al. Assessing the quality of proton PBS treatment
533 delivery using machine log files: comprehensive analysis of clinical treatments delivered at
534 PSI Gantry 2. *Phys Med Biol*. 2016;61(3):1171-1181. doi:10.1088/0031-9155/61/3/1171
- 535 11. Li H, Sahoo N, Poenisch F, et al. Use of treatment log files in spot scanning proton therapy as
536 part of patient-specific quality assurance. *Med Phys*. 2013;40(2):021703.
537 doi:10.1118/1.4773312
- 538 12. Russo G, Attili A, Battistoni G, et al. A novel algorithm for the calculation of physical and
539 biological irradiation quantities in scanned ion beam therapy: the beamlet superposition
540 approach. *Phys Med Biol*. 2016;61(1):183-214. doi:10.1088/0031-9155/61/1/183
- 541 13. Low DA, Harms WB, Mutic S, Purdy JA. A technique for the quantitative evaluation of dose
542 distributions. *Med Phys*. 1998;25(5):656-661. doi:10.1118/1.598248
- 543 14. Rossi S. The National Centre for Oncological Hadrontherapy (CNAO): Status and
544 perspectives. *Phys Medica*. 2015;31(4):333-351. doi:10.1016/j.ejmp.2015.03.001
- 545 15. Giordanengo S, Palmans H. Dose detectors, sensors, and their applications. *Med Phys*.
546 2018;45(11):e1051-e1072. doi:10.1002/mp.13089
- 547 16. Elsässer T, Weyrather WK, Friedrich T, et al. Quantification of the relative biological
548 effectiveness for ion beam radiotherapy: Direct experimental comparison of proton and carbon
549 ion beams and a novel approach for treatment planning. *Int J Radiat Oncol Biol Phys*.
550 2010;78(4):1177-1183. doi:10.1016/j.ijrobp.2010.05.014
- 551 17. Flanz J. Particle Beam Scanning. In: Paganetti H, ed. *Proton Therapy Physics*. CRC Press;
552 2018:169-206.

- 553 18. Badura E, Brand H, Essel HG, et al. Control system for cancer therapy with a heavy ion beam
554 at GSI. *IEEE Trans Nucl Sci.* 2000;47(2):170-173. doi:10.1109/23.846141
- 555 19. Grözinger SO, Bert C, Haberer T, Kraft G, Rietzel E. Motion compensation with a scanned
556 ion beam: a technical feasibility study. *Radiat Oncol.* 2008;3:34. doi:10.1186/1748-717X-3-
557 34
- 558 20. Psoroulas S, Bula C, Actis O, Weber DC, Meer D. A predictive algorithm for spot position
559 corrections after fast energy switching in proton pencil beam scanning. *Med Phys.*
560 2018;45(11):4806-4815. doi:10.1002/mp.13217
- 561 21. Furukawa T, Hara Y, Mizushima K, et al. Development of NIRS pencil beam scanning system
562 for carbon ion radiotherapy. *Nucl Instruments Methods Phys Res Sect B Beam Interact with*
563 *Mater Atoms.* 2017;406:361-367. doi:10.1016/j.nimb.2016.10.029

564

565